Algerian Journal of Environmental Science and Technology
June edition. Vol.9. N°2. (2023)
ISSN : 2437-1114
www.aljest.org

Instrumental neutron activation and spectroscopic elemental analysis of iron-rich ore from Gara Djebillet region in Algeria

N. Sabba [1], N. Sahraoui[1], I. Ammour[1], A. Hadri [2], C. Aziez [3], B. Saim [4], B. Guedioura [4]

[1] Laboratory of valorization and recycling of matter's and sustainable development, Faculty of Mechanical Engineering and Process Engineering USTHB, BP 32, Algiers, Algeria
[2] Reactor Division, Nuclear Research Center, Draria, Algeria
[2] Physics and Application division, Nuclear Research Center, Draria, Algeria
[3] Radiation protection and Safety division, Nuclear Research Center, Draria, Algeria
[4] Reactor Division, Nuclear Research Center, Draria, Algeria

*Corresponding author: nassilasabba@yahoo.fr

ARTICLE INFO

Article History :

Received ***: 26/09/2022***
Accepted ***: 31/10/2022***

***Key Words*:**

Oolitic iron ore, mineralogy; Microstructure; Neutron activation analysis; Spectroscopy.

ABSTRACT/RESUME

Abstract: *This study was aimed at determining the concentrations of all chemical elements in iron-rich ore from the Gara Djebillet region in Algeria using instrumental neutron activation and spectroscopic analysis. **S**amples from four sites in the region were analyzed by spectroscopic methods such as X-ray diffraction (XRD), X-ray fluorescence (XRF) and scanning microscopy (SM). In addition, instrumental neutron activation analysis (INAA) allowed for a complete quantitative characterization of the ore. Results showed that there were forty-two elements found in trace and ultra-trace amounts and which were equally exploitable. The iron-rich deposits of the region are of great economic value to the country.*

I. Introduction

Oolitic iron ores of high phosphorus are widely distributed globally including large-scale deposits [1-3]. The Devonian ferruginous formation of the Tindouf basin in the Algerian western Sahara (Figure 1) was discovered in 1952 [3, 4]. The Basin is oriented WSW-ENE, bounded in the north by the Anti-Atlas, the south by the Reguibat Shield, the west by the Mauritanides and the east by the Erg Chech Depression. The iron ore deposit in the Gara Djebilet region of the basin has been estimated at more than 2.65 billion tonnes of grade 53-58 % Fe [5, 6]. Furthermore, the Ministry of Energy and Mining of Algeria has also reported large quantities iron ore at Gara Djebilet and nearby Mechri Abdelaziz [7, 8].

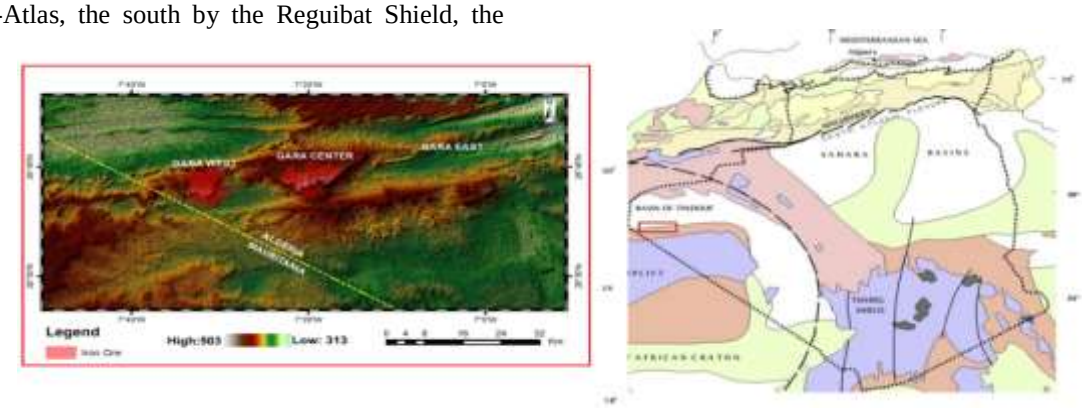

Figure 1. *Iron ore index of Gara Djebilet. Iron ore (red), and all other formations (green)* [6].

Efficient iron ore processing operations depends on a detailed knowledge of the chemical and mineralogical distribution as well as impurities content of the raw material. Techniques such as X-

ray Diffraction (XRD), Scanning Electron Microscopy (SEM) are common tools utilized in the characterisation of iron ores (Sarjoughian et al., 2020). Neutron activation analysis in its instrumental form (INAA) is a simple method of analysis, involving two separate processes, excitation and measurement [9-12].

The excitation of samples by exposure to neutrons, as well as the subsequent measurement of the induced activity by a suitable detector, are based on physical laws, giving an accurate value for the quantity of a specific element in the sample [13, 14]. This technique is physically non-destructive; induced radio-activities cannot be decreased to the background level even after a reasonable cooling interval time if samples are subjected to long term irradiation. The method can be applied to most sample matrices without any pre-treatment. Whilst, the INAA analysis has high sensitivity and good precision and being very useful for specific multi element evaluation with very low detection limits in the sub-ppm range [15, 17].

II. Materials and methods

II.1. Scanning Electron Microscopy

In order to obtain an adequate particle size for our different analyses, 5 Kg of for four different samples iron ores were ground to less than 150 µm and further ground in a FRITSCH mortar grinder before analysis by SEM/EDS and X-ray diffraction. For the other analytical methods (i.e. XRD and INAA), the crushed material was further homogenized using a TRIAXE® mixer, and sieved through a 100 µm mesh. Furthermore, the external morphologies of Gara-Djebilet iron ores were examined with the ESEM XR30 coupled to an auxiliary station for energy-dispersive X-ray installed at Algiers Nuclear Research Centre.

II.2. X-Ray diffraction

The degree of crystallinity of iron ores powder was assessed by using a PHILIPS instrument, model X-pert XRD at a scan range 2θ from 2 to 80°, operating at 40 kV, and using a Cu radiation source. The scans were obtained using a scan step size of 0.03° with a scan step time of 0.25 s.

II.3. X-Ray fluorescence

The X-ray fluorescence analysis of the studied samples was performed using Niton XL3t GOLDD+ portable spectrometer, utilized for the analysis of powder simples of rocks, minerals, ores, and concentrates. The spectrometer was equipped with a miniaturized Ag anode X-ray tube (50 kV, 200 µA). Equipped with a high-performance detector Geometrically Optimized Large Area Drift Detector (GOLLD), was able to recording spectra at high count rates. The normal measuring head/aperture of this device was 8 mm in diameter, which could be reduced to 3 mm using a built-in spot collimator. The time of accumulation of X-Ray fluorescence spectra was 30 s per sample.

II.3. Instrumental neutron activation analysis

The irradiation for the INAA was carried out in NuR research reactor of the Draria Nuclear Research Center (CRND) Algeria. Three sub-samples, each containing ~50-100 mg of iron ores powder, two standard elements, and blanks, were weighted, heat-sealed in polyethylene, and then packed in high density polyethylene capsule material.

For the determination of the short half live radioelements, the samples were irradiated for 100 s in a thermal column at the neutron flux magnitude 5.4 × 1012 n cm-2 s-1. The subsequent irradiations were performed under 2.4 x 1013 n cm-2 s-1 for hours. Thence, after the second irradiation and two days cooling time, the iron ores samples were analysed for selecting the long lived elements. Four weeks cooling time was subsequently required to decrease the residual activity allowing for measurements of the long-lived elements.

After a cooling time for each radio nuclide, an γ-ray spectrum was acquired. Samples and standards were placed in close geometry using a solid-state Canberra GEM409 P Germanium detector. After irradiation the covers were removed, and the samples were mounted on standard Plexiglas plates. They were assayed for γ-activity of the activation products using an HPGe detector coupled to a PC based 4K analyser in an efficiency calibrated position with reproducible sample-to-detector geometry. The sample-to-detector distance was maintained at 10-15 cm depending upon the level of activity to avoid true coincidences effects. The detector system had a resolution of 1.8 keV at 1332 keV. The activities of radionuclides were considered as a function of time to ensure purity and identity. The Gamma-ray standard of Eu52 was used for efficiency calibration of the detector, at different distances between the sample and detector in a stable source-to-detector geometry. The γ-ray spectra analysis was carried out by using the appropriate computing software. The computations were done using the comparative method of INAA **(Equation 1)** [9]. for element 'i'. The concentration of element 'i' was denoted by C:

$$C_{i,samp} = C_{i,std} \frac{cps_{i,samp}}{cps_{i,std}} \frac{D_{std}}{D_{samp}} \frac{\rho_{std}}{\rho_{samp}} \quad (1)$$

where $D = e^{-\lambda t_d}$ the decay time factor and $\rho = \left(\frac{1-e^{-\lambda t_{rt}}}{\lambda t_{lt}}\right)$ the counting factor for the decay during counting, λ the decay constant, and t_d, t_{rt} and t_{lt} the decay time, real time, and live time of counting, respectively. The detection limit of INAA was

based on the signal-to-noise ratio, the selectivity of determining with a certain degree of confidence a peak in the gamma-ray spectrum. The photo-peak in the spectrum of the γ-ray emission by the radionuclide of interest was the 'signal'. The 'noise' results from the detection of photons from the ambient background value B, from the Compton continuum due to the interaction of higher energy γ-rays. The detection limit DL depended on the irradiation, the decay, and the counting conditions. According to Equation 2 [9].

$$D_L = 2.71 + 4.65\sqrt{B} \quad \textbf{(2)}$$

Validation of the technique was done by irradiating two standards reference materials together IAEA-336 [18] and National reference materials of stream sediment N°- GBW07312 of China [19].

II.3. Quality control procedures

To evaluate the accuracy and the performance of the assay, the Z- score is most often used and biological reference materials were analysed, i.e., tulip sample (IPE-175) and lichen (IAEA-336), the former being used as control and the latter as a comparator.

So, the Z- score was calculated according to Equation 3 [20, 21]:

$$Z\text{-}score = (X-\mu)/\sigma \quad \textbf{(3)}$$

where X is the observed value, μ the certified value and σ its standard deviation. The Z-scores were used to test the quality of the results. If $|Z| \leq 3$, the experimental value was considered as acceptable, $2 < |Z| < 3$, was questionable and $|Z| \geq 3$, was considered not acceptable [22, 23].

III. Results and discussion

III.1. SEM/EDX analysis

As shown in Figure 2a, two phases were present as represented by black and grey with a similar composition according to EDX analysis. These forms can be considered as oolites which seems to be identical to those of nubecularia generally known in the phosphate or carbonate phases. Moreover, it was noticed that the streamlined parts are relatively aligned in the longitudinal direction of the section. Besides, different SEM/EDX spectra were seen within a section of the Gara Djebilet iron ores samples indicated by upper (dark) and lower (light) areas in Figure 2b and 2c . The corresponding quantitative data on the dark and light/bright areas of the Gara-Djebilet iron ores samples are presented in Table 1. The results show a clear difference in the quantitative elemental composition (i.e., peak heights) between these two areas.

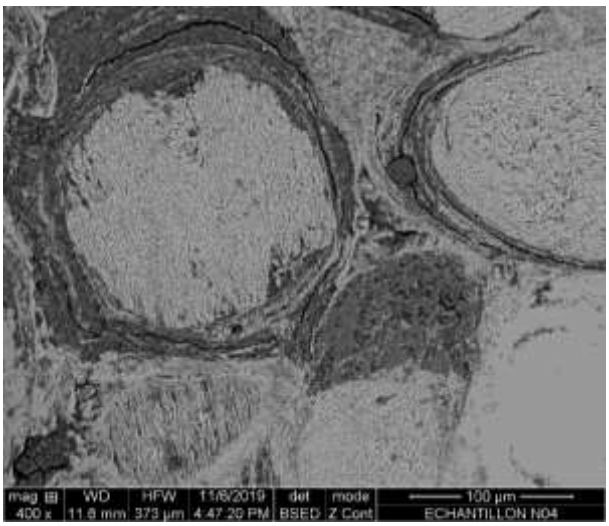

Figure 2a. *Photomicrographs of iron ores samples*

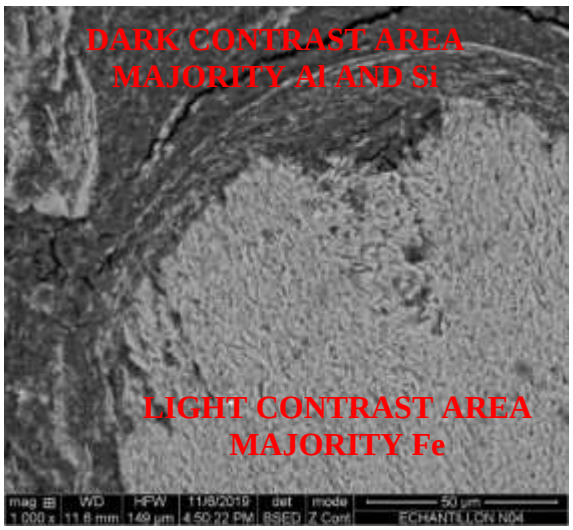

Figure 2b. *. Photomicrograph showing sampling area*

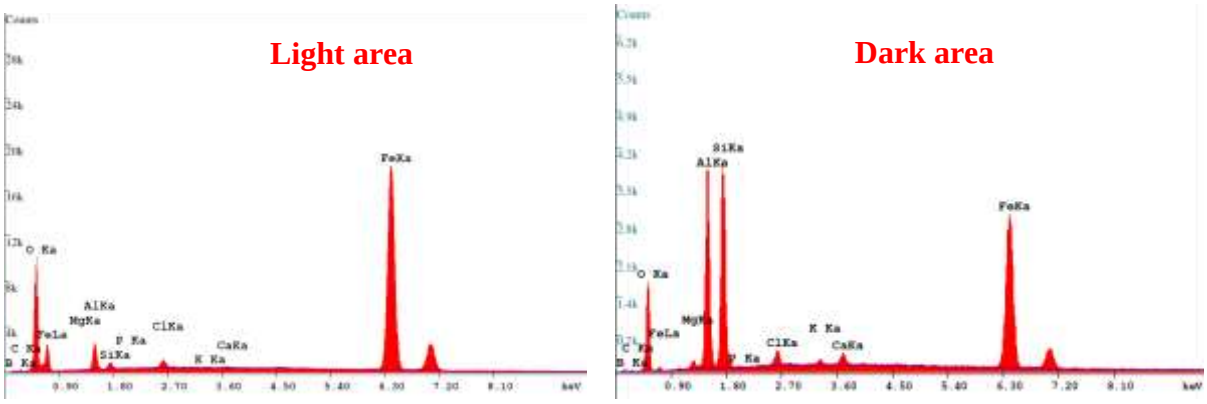

Figure 2c. *EDX spectrum*

Table 1. *Elemental composition of iron ores samples obtained by SEM/EDX.*

Elements	Dark contrast area (W %)	Bright/Light contrast area (W %)
B	5.63	3.85
C	0.33	0.72
O	15.92	18.69
Mg	0.68	0.01
Al	15.04	3.19
Si	15.82	0.66
P	0.1	0.05
Cl	1.33	0.79
K	0.47	0.03
Ca	1.11	0.13
Fe	43.57	71.90

III.2. X-Ray Fluorescence

Based on the chemical compositions, the ore samples namely TFe (23.6%) and P (0.32%) are considered highly phosphorus. The results of the X-ray fluorescence analysis yield the chemical composition in detectable elements. According to Table 2, the composition of 0.82% by weight of the sample is unknown.

Table 2. *Chemical composition of raw samples by XRF.*

Elements	%wt
TFe	23.6
Si	6.7
Al	5
P	0.32
Cl	0.51
Ca	9.46
K	0.16
Mg	0.73
S	0.12
Ba	0.25
Ti	0.21
LoL	0.82

III.3. X-Ray diffraction

As depicted in Figure 3, X-ray diffraction also revealed the different elements. Iron was found in the form of magnetite (peak 3), hematite (peak 1), magnetite (peak 3) and goethite (peak 2). There were other complex phases (i.e., smaller peaks), probably based on iron with other elements. Indeed, the results indicate that the gangue contains mainly kaolinite and quartz. However, the amorphous mineralogical phases of phosphorus and aluminium do not appear. Unfortunately, the rare earths present a small quantities, could not be identified by X-rays neither nor by XRF.

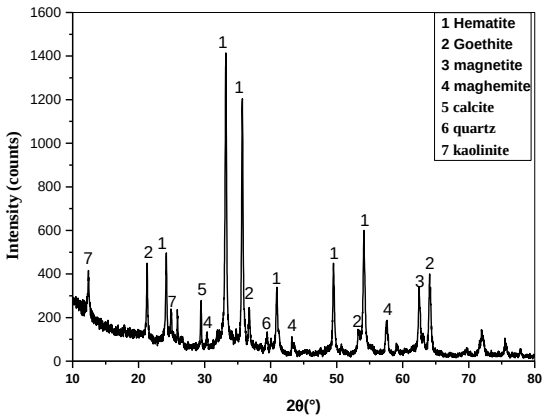

Figure 3. *DRX spectrum of Gara-Djebilet iron ores.*

III.3. Instrumental neutron activation analysis

The concentrations of 14 elements obtained using instrumental neutron activation analysis (IAEA-336) were found to be in good agreement with certified values of the elements, indicating good accuracy of the technique. Comparison between the current measured data and the reference materials IAEA-336 [23] and GBW07312 [22] are summarized in Table 3. The standard deviations and the computed Z-scores were also included. The Z-scores for most elements were found to be within ± 2, ensuring the reliability of the elemental concentrations to be within ± 10%.

Table 3. *Elemental concentrations (µg/g) in the current iron or samples and reference material IAEA-336 obtained by INAA method.*

Element	Certified value	This work	Z-score
Ti	50.1±20.2	48.9±16.2	0.06
V	1.47±0.16	1.44±0.12	0.18
Zn	30.3±4.5	32.8±3.18	-0.55
Al	675±143	679±101	-0.03
As	0.63±0.07	0.66±0.05	-0.38
Ba	6.39±1.29	6.11±1.1	0.21
Cr	1.06±0.29	1.21±0.98	-0.51
Cu	3.6±0.7	3.9±0.8	1
Co	0.29±0.06	0.42±0.02	-2.1
Fe	428±53	487±45	-1.1
Mn	63.4±6.9	67.1±3.6	-0.5
Rb	1.76±0.19	1.59±0.07	1
Sb	0.07±0.01	0.08±0.01	-1
Se	0.22±0.04	0.23±0.04	-0.2

A fragment of a sample gamma spectrum recorded by hyper pure germanium detector two weeks after the irradiation is shown in Figure 4. The gamma spectrum obtained covers the energy band between [0, 1500] keV. For better clearness, we have opted for dividing the energy axis into four bands where the γ peaks are clearly observed. The presence of specific radioisotopes is painted in the γ spectra figures 4 (a), 4(b), 4(c), 4(d). The medium and long elements such as Cd, Np, Yb, Lu, Eu, Ta, Tb, Pa, Cr, Hf, Ga, Sc, Co, and Fe have been identified. Each radioelement was identified using gamma-vision software (Vision, Gamma. (2003). In principle, every observable peak can be used for the determination of the corresponding element. However, as can be seen in Figure 4, a judicious choice of the most appropriate peak may contribute much better to the obtainable accuracy and precision.

Table 4 groups the detailed results obtained by different analyses of Gara-Djebilet deposit iron ores, including the average concentrations along with the standard deviations. Each value is the average of the results obtained with three different samples, for each sampling site.

A comparison of iron concentration yielded the following profile of samples. Site-1 (71%) > Site-2 (60%) > literature (50%) > Site-3 (43%) > Site-4 (37%). It seemed that Site 3, 4 and literature were medium grade iron ores. The rare earth elements (REEs) are important tracers and used in modelling of various geochemical processes (Tsai and Yeh 1997). So, by comparing the results obtained by INAA on site-3 to those published elsewhere for samples having an identical iron content (Wasim. M, et al; 2020), 10 REEs measured in site-3, their average concentrations were 37.6, 82.0, 346, 9.52, 0.07, 2.15, 0.21, 14.2, 6.63, 5.11 (µg/g) for La, Ce, Nd, Sm, Eu, Gd, Tb, Dy, Yb, and Lu, respectively. Really, a comparison of the mass fractions of REEs found in our study, were higher in the Gara Djebilet deposit iron ores than those published in literature (Wasim. M, et al; 2020). Although the most intense peaks guaranteed the highest precision, some of them should be avoided, because they interfered with peaks of other isotopes of different chemical elements, resulting in systematic errors. On the other hand, for a single isotope, those peaks free from interferences should not be used to calculate the concentrations averaged over all peaks. The operational range of INAA extends from ultra-trace (ng/g) to percentage level (%). There is, however no rule defining a threshold concentration above which the term trace must be used. The notion of trace does not have the same meaning depending on whether one is in the fields of nuclear, geology, biology, metallurgy, exploitation of iron deposits, etc. [24]. We may thus establish the following classification for a given analysed elemental mass depending on its concentration m (µg/g) i.e. for mass fraction m > 5000, the elemental mass is called main element, 5000 < m < 500 (minority), m < 500 (trace) and m < 50 (ultra-trace).
The compilations of measurement results for all sites are given in Table 4.

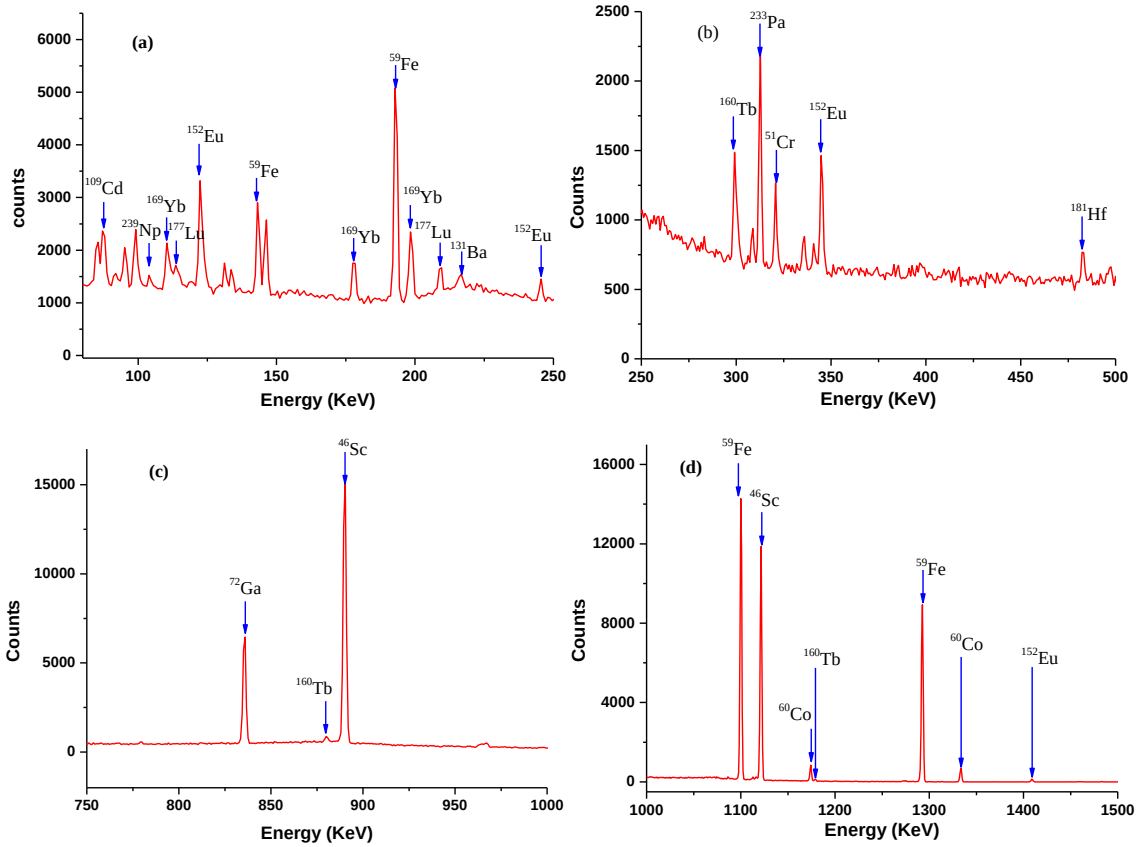

Figure 4. *A γ-Ray spectrum of Gara-Djebilet deposit iron ores sample, for energy intervals: (a) [80-250] keV, (b) [250-500] keV, (c) [750-1000] keV, (d) [1000-1500]*

Table 4. *Elemental mass fraction in (µg/g) or otherwise, in four different deposit iron ores sites. Uncertainties are standard deviations of independent measurements*

1- Majority elements (% ± σ*)

Analyzed element	Site-1	Site-2	Site-3	Site-4	Literature**
Al	9.35± 2.67	5.32± 0.45	4.35± 1.06	5.08± 0.79	3.43± 0.25
K	1.11± 0.31	0.37± 0.01	0.24± 0.1	0.18± 0.03	0.60± 0.05
Mg	4.7±1. 93	1.15± 0.44	0.66± 0.24	0.43± 0.02	0.020 ±0.00 1
Na	0.21± 0.01	0.076 ±0.00 3	0.05± 0.005	0.19± 0.002	0.010 ±0.00 1
Fe	71±3	59.8± 3.1	42.76 ±1.63	37±9	49.9± 0.9

2- Minority elements (µg/g ± σ*)

Element	Site-1	Site-2	Site-3	Site-4	Literature**
Mn	7232± 135	2010± 22	1236±7 7	612±25	204 ±5
Ti	6244± 1951	2309± 221	1849±3 2	1518±6 08	300 ±20
V	752±9 2	714±2 1	400±32	173±5	12.8 ±1.2
As	2096± 593	< D.L	290±17	56.38±2 2.74	3.9± 0.3
Ba	723±2 61	< D.L	68±13	590±37 0	103 ±8
Cd	6022± 1597	< D.L	8.71±1. 44	815±40	N.R
Ga	141±1 7	10.08 ±0.73	35.41±1 0.29	1.34±0. 35	N.R
La	123±4 8	32.09 ±0.93	37.57±1 .78	57.75±3 .17	34.9 ±3.1
Mo	971±1 58	6.99± 3.04	1.71±0. 01	264±49	N.R
Nd	437±1 17	< D.L	346±1	43.47±8 .12	<D. L
Rb	597±3 47	142±0 .78	17.41±2 .72	690±79	34.0 ±3.0
Zn	7030± 2800	85±18	91±9	5787±8 63	38.2 ±4.2
Zr	3588± 1754	537±1 82	18.67±5 .47	2887±5 76	N.R

3- Trace elements (µg/g ± σ*)

Element	Site-1	Site-2	Site-3	Site-4	Literature**
Dy	23±1.24	23.11 ±0.13	14.19 ±1.1	12.97 ±0.35	<D.L
In	5.56± 0.21	1.52± 0.08	0.92± 0.1	0.47± 0.03	<D.L
Br	35.17 ±13.48	0.74 ±0.46	0.56± 0.31	8.58± 4.11	N.R
Ce	122.23±51	< D.L	82±5	124±36	10.7±1.3
Co	30.69 ±7.75	4.35± 1.7	3.82± 0.63	19.55 ±3.9	6.4±0.4
Cr	64.12 ±33.04	< D.L	80±14	22.89 ±2.16	130±0.6
Cs	45.3± 7.07	< D.L	10.85 ±1.84	35.14 ±7.95	8.1±0.6
Eu	60.74 ±8.24	12.11 ±9.33	0.07± 0.01	24.56 ±3.12	0.060± 0.004
Tb	34.93 ±8.24	0.29± 0.08	0.21+ 0.05	5.73± 0.66	<D.L
W	31.53 ±6.9	1.57± 0.14	90.08 ±9.73	1.44± 0.92	<D.L

4- Ultra-trace elements (µg/g ± σ*)

Element	Site-1	Site-2	Site-3	Site-4	Literature**
Ag	12.89 ±7.27	5.54± 0.45	0.91±1.65	2.08±0.83	**N.R**
Gd	9.65± 3.25	17.82 ±1.91	2.15±0.21	34.07± 6.05	**N.R**
Hf	18.83 ±3.49	0.91± 0.3	158±85	5.69±2.15	**7.50**
Lu	1.53± 0.11	3.65± 0.31	5.11±0.51	2.88±0.11	**0.24± 0.02**
U	5.61± 1.01	4.14± 0.63	3.36±0.82	3.27±0.14	**8.3±0.6**
Nb	17.4± 0.46	9.56± 6.31	3.64±0.51	62.48± 2.02	**<D.L**
Sb	10.15 ±0.46	< D.L	8.39±1.65	32.61± 3.09	**10.6± 1.1**
Sc	21.96 ±2.82	20.36 ±1.31	29.36± 2.72	11.15± 4.14	**3.1±0.3**
Sm	22.57 ±3.49	< D.L	9.52±2.28	15.97± 1.01	**1.30± 0.09**
Ta	25.57 ±10.47	1.11± 0.25	5.22±4.32	14.44± 4.84	**<D.L**
Th	17.68 ±6.49	6.26± 2.53	5.8±0.84	20.35± 4.36	**<D.L**
Yb	12.8± 5.72	< D.L	6.63±1.59	7.54±1.34	**1.60± 0.01**

*Uncertainties are standard deviations of independent measurements; **Results obtained from literature: [25]; Site 1: Gara-Djebilet East (1 m in deep); Site 2: Gara-Djebilet East (Surface sampling); Site 3: Gara-Djebilet Center (Surface sampling); Site 2: Gara-Djebilet West (Surface sampling); D.L: Detection Limit, N.R: No Result.

IV. Conclusion

Structural and elemental analytical characterisation of Gara-Djebilet iron ores deposits were succesfully analyzed by Scanning Electron Microscope coupled to station Energy Dispersive X-ray Spectroscopy (SEM-EDS), X-ray diffraction (XRD), X-ray fluorescence (XRF) and Instrumental Neutron Activation Analysis (INAA). The SEM-EDS assessment showed the existence of two phases in the iron ore represented by black and bright/light contrast with similar composition according to X-ray energy dispersive micro analysis. However the bright/light contrast areas were found to have an iron content ~72%, while black contrast areas have an iron content of ~44%. Whilst, the XRD allowed for the elemental identification of the phases. Indeed, the iron was found in the form of magnetite, hematite, maghemite and goethite. On the other hand, the XRF analysis was also employed for comparing and detecting elements such as P, C, Si, and Pb that can only be seen with this technique. Finally, the instrumental neutron activation analysis indicated that there were 42 elements in the deposit iron ores samples collected from sites in Gara-Djebilet area in south west Algeria. The elements included the major, minor, trace and ultra-trace elements. In addition, the rare earth elements, included actinides elements uranium and thorium. The iron-rich deposits of the region are of great economic value to the country. This research is our contribution to the understanding of the elemental composition of the Gara-Djebilet deposit iron ores and also to establishing a data base for further use in the future.

Acknowledgments

The authors are thankful to the teams of the operating department, the radiation protection department and the team of the neutron activation analysis laboratory for their cooperation during the realisation of our research work.

V. References

1. Quast, K. A. Review on the characterisation and processing of oolitic iron ores. *Minerals Engineering*, 126 (2018) 89-100.
2. Baioumy, H.; Omran, M.; Fabritius, T. Mineralogy, geochemistry and the origin of high-phosphorus oolitic iron ores of Aswan, Egypt. *Ore Geology Reviews*. 80 (2017)185-199.
3. Li, K.-Q.; Ni, W.; Zhu, M. ; Zheng, M.-J. ; Li, Y. Iron extraction from oolitic iron ore by a deep reduction process. *Journal of iron and steel research international*. 18 (2011) 9-13. 317-323.
4. Champetier, Y.; Hamdadou, E.; Hamdadou, M. Examples of biogenic support of mineralization in two oolitic iron ores—Lorraine (France) and Gara Djebilet (Algeria). *Sedimentary Geology*. 5 (1987) 249-255.
5. Guerrak, S. Geology of the Early Devonian oolitic iron ore of the Gara Djebilet field, Saharan Platform, Algeria. *Ore Geology Reviews*.3 (1988) 333-358.
6. Bersi, M.; Saibi, H.; Chabou, M. C. Aerogravity and remote sensing observations of an iron deposit in Gara Djebilet, southwestern Algeria. *Journal of African Earth Sciences*. 116 (2016) 134-150.
7. Ciampalini, A. ; Garfagnoli, F. ; Del Ventisette, C. ; Moretti, S. Potential use of remote sensing techniques for exploration of iron deposits in Western Sahara and Southwest of Algeria. *Natural resources research*. 22 (2013) 179-190.
8. Ciampalini, A. ; Garfagnoli, F. ; Antonielli, B. ; Moretti, S. ; Righini, G. Remote sensing techniques using Landsat ETM+ applied to the detection of iron ore deposits in Western Africa. *Arabian Journal of Geosciences*. 6 (2013) 4529-4546.
9. Silachyov, I. Y. Combination of Instrumental Neutron Activation Analysis with X-Ray Fluorescence Spectrometry for the Determination of Rare-Earth Elements in Geological Samples. *Journal of Analytical Chemistry*. 75 (2020) 878-889.
10. Sarjoughian, F.; Habibi, I.; Lentz, D. R.; Azizi, H.; Esna-Ashari, A. Magnetite compositions from the Baba Ali iron deposit in the Sanandaj-Sirjan zone, western Iran: Implications for ore genesis. *Ore Geology Reviews*.126 (2020) 103728.
11. Bitewlign, T. A.; Chaubey, A. K.; Beyene, G. A.; Melikegnaw, T. H.; Mizera, J.; Kameník, J.; Krausová, I.; Kučera, J. Instrumental neutron activation analysis of environmental samples from a region with prevalence of population disabilities in the North Gondar, Ethiopia. *Journal of Radioanalytical and Nuclear Chemistry*. 311 (2017) 2047-2059.
12. Greenberg, R. R.; Bode, P.; Fernandes, E. A. D. N. Neutron activation analysis: a primary method of measurement. *Spectrochimica Acta Part B: Atomic Spectroscopy*. 66 (2011) 193-241.
13. Samanta, S. K.; Nag, T. N. ; Sharma, V. ; Tripathi, R. ; Acharya, R. ; Pujari, P. K. Intercomparison studies of Instrumental Neutron Activation Analysis using singles and gamma–gamma coincidence spectrometry for trace element determination in sodalime glass and sediment matrices and utilization of coincidence method for rapid automobile glass forensics. Nuclear Instruments and Methods in Physics Research Section A: Accelerators, Spectrometers, *Detectors and Associated Equipment*. 1006 (2021) 165429.
14. Guinn, V.; Wagner, C. Instrumental neutron activation analysis. *Analytical Chemistry*. 32(1960)
15. Thien, B. N.; Ba, V. N.; Man, M. T.; Loan, T. T. H. Analysis of the soil to food crops transfer factor and risk assessment of multi-elements at the suburban area of Ho Chi Minh city, Vietnam using instrumental neutron activation analysis (INAA). *Journal of Environmental Management*. 291 (2020) 112637.
16. Sergeeva, A.; Zinicovscaia, I.; Grozdov, D. ; Yushin, N. Assessment of selected rare earth elements, HF, Th, and U in the Donetsk region using moss bags technique. *Atmospheric Pollution Research*. 12 (2021) 101165.
17. Glascock, M. D.; Neff, H.; Vaughn, K. J. Instrumental neutron activation analysis and multivariate statistics for pottery provenance. *Hyperfine Interactions*. 154 (2004) 95-105.
18. Heller-Zeisler, S.; Zeisler, R.; Zeiller, E.; Parr, R.; Radecki, Z.; Burns, K. ; DE Regge, P. Report on the intercomparison run for the determination of trace and minor elements in lichen material. IAEA-336. *International Atomic Energy Agency*. (1999).
19. Wang, X.; Shi, Z.; Shi, Y. ; Ni, S. ; Wang, R. ; Xu, W. ; Xu, J. Distribution of potentially toxic elements in sediment of the Anning River near the REE and V-Ti magnetite mines in the Panxi Rift, SW China. *Journal of Geochemical Exploration*. (2018) 184, 110-118.
20. Datta, J.; Chowdhury, D.; Verma, R.; Reddy, A. Determination of elemental concentrations in environmental plant samples by instrumental neutron activation analysis. *Journal of Radioanalytical and Nuclear Chemistry*. 294(2012) 261-265
21. Bode, P.; Van Dijk, C. Operational management of results in INAA utilizing a versatile system of control charts. *Journal of radioanalytical and nuclear chemistry*. 215 (1997) 87-94.
22. Acharya, R.; Swain, K.; Kumar, A.; Ajith, N.; Verma, R.; Reddy, A. Determination of k 0-factors and validation of k 0-INAA for short-lived nuclides. *Journal of radioanalytical and nuclear chemistry*.286 (2010) 286, 507-511.
23. Pignata, M.; Plá, R. ; Jasan, R.; Martinez, M. ; Rodriguez, J. ; Wannaz, E. ; Gudino, G. ; Carreras, H. ; González, C. Distribution of atmospheric trace elements and assesment of air quality in Argentina employing the lichen, Ramalina celastri, as a passive biomonitor: detection of air pollution emission sources. *International Journal of Environment and Health*. 1 (2007)29-46.
24. Smodiš, B.; Barradas, N. P.; Ridikas, D.; Bode, P.; Landsberger, S. An E-learning tool as living book for knowledge preservation in neutron activation analysis. *Journal of Radioanalytical and Nuclear Chemistry*. 325 (2020) 737-741.
25. Wasim, M.; Tariq, A. ; Shafique, M. A. ; Qureshi, R. N. Characterization and differentiation of iron ores using X-ray diffractometry, k0 instrumental neutron activation analysis and inductively coupled plasma optical emission spectrometry. *Journal of Radioanalytical and Nuclear Chemistry*, 323(1) (2020) 179-187.

Please cite this Article as:
Sabba N. , Sahraoui N., Ammour I., Hadri A. , Aziez C., Saim B. , Guedioura B., Instrumental neutron activation and spectroscopic elemental analysis of iron-rich ore from Gara Djebillet region in Algeria, ***Algerian J. Env. Sc. Technology***, **9:2 (2023) 3170-3177**